

Seismic Behavior of Wood Diaphragms in Pre-1950s Unreinforced Masonry Buildings

David F. Peralta¹; Joseph M. Bracci²; and Mary Beth D. Hueste³

Abstract: This paper documents an experimental testing program on the lateral in-plane behavior of pre-1950s existing and rehabilitated wood floor and roof diaphragms in unreinforced masonry buildings found in the Central and Eastern regions of the United States. Three diaphragm specimens were constructed with elements and connection details typical of pre-1950s construction. The specimens were tested, retrofitted, and retested again using different rehabilitation methods, including enhanced shear connectors and perimeter strapping, a steel truss attached to the bottom of the joists and connected to the vertical lateral force resisting system, and unblocked and blocked plywood overlays connected to the sheathing and joists. Specimens were tested under quasi-static reversed cyclic loading to evaluate their in-plane lateral deformation performance at selected locations of the diaphragm. The measured in-plane lateral response was used to develop backbone curves defining the relationship between the applied lateral force and the diaphragm midspan displacement. These backbone curves provide the basis for bilinear curves that define yield strength and displacement, effective stiffness, and post-yield stiffness. These parameters, based on experimental testing, were compared with the provisions for wood diaphragms in the FEMA guidelines for seismic rehabilitation of buildings (FEMA 273 and its update FEMA 356). For the diaphragms tested, FEMA 273 tended to overpredict the stiffness and significantly underpredict yield displacement and ultimate deformation levels, while FEMA 356 tended to underpredict stiffness and overpredict yield displacement. However, the updated FEMA 356 guidelines tend to conservatively estimate the diaphragm response in terms of strength, stiffness, and deformability.

DOI: 10.1061/(ASCE)0733-9445(2004)130:12(2040)

CE Database subject headings: Diaphragms; Wood floors; Seismic response; Connections, bolted; Experimental data; Rehabilitation.

Introduction

Diaphragms are horizontal, or nearly horizontal, structural elements used to distribute lateral forces to the vertical elements of lateral force resisting systems. In unreinforced masonry (URM) buildings, the two basic structural components to resist lateral forces are (1) the horizontal diaphragms of the building (floors and roof) and (2) the URM walls, which distribute the lateral forces to the foundation level. The use of wood floors and roofs in masonry buildings is quite common in both past and current construction. Wood diaphragms are an assemblage of elements that typically include three components: sheathing, framing, and chords. Buildings constructed prior to 1945 generally do not have plywood sheathing on the floors or roof. In addition, the use of chords was not common. Sheathing in these buildings generally consisted of straight or diagonal sheathing boards nailed to the framing (ATC 1997a). The framing members that support the

sheathing were composed of joist members supported vertically on the masonry wall and laterally by cross-bridging members. Bridging was typically made of short wood boards that were set nailed diagonally between joists to form an "X" pattern perpendicular to the joists. Joist ends were cut diagonally (firecut) and supported in pocket holes in the masonry wall, having a bearing support of approximately 76 mm. Typical pre-1950s URM buildings in the St. Louis area had iron wall anchors (star or government anchors) at approximately every fourth joist, which were used to connect the diaphragm and the supporting wall.

The lateral in-plane behavior of wood floor and roof diaphragms in URM buildings has important seismic implications for the Midwest region of the United States, which has experienced some of the strongest earthquakes in the history of the country caused by activity on the New Madrid seismic zone (Stelzer 1999). This study focuses on essential facility buildings because of their importance immediately after a seismic event. In particular, structures constructed prior to 1950 were emphasized because they are generally considered to be at greater risk during a seismic event compared to more modern buildings. From information gathered in the St. Louis area, most firehouses constructed prior to 1950 have diaphragms composed of nailed wood decking on wood joists. An example of a pre-1950s URM firehouse in St. Louis is shown in Fig. 1.

Several construction details that make URM buildings vulnerable during earthquakes have been identified in past earthquakes. These details include a lack of chord members along the edges of the diaphragm and insufficient connections between the diaphragm and the perimeter masonry walls (see Fig. 2). After the occurrence of the 1994 Northridge earthquake in California, it was found that the major source of damage in reinforced masonry

¹Engineer, Unitech Consulting Engineers, Inc., 12758 Cimarron Path, Suite 118, San Antonio, TX 78249.

²Associate Professor, Dept. of Civil Engineering, Texas A&M Univ., College Station, TX 77843-3136.

³Assistant Professor, Dept. of Civil Engineering, Texas A&M Univ., College Station, TX 77843-3136.

Note. Associate Editor: Gregory A. MacRae. Discussion open until May 1, 2005. Separate discussions must be submitted for individual papers. To extend the closing date by one month, a written request must be filed with the ASCE Managing Editor. The manuscript for this paper was submitted for review and possible publication on June 2, 2003; approved on May 6, 2004. This paper is part of the *Journal of Structural Engineering*, Vol. 130, No. 12, December 1, 2004. ©ASCE, ISSN 0733-9445/2004/12-2040-2050/\$18.00.



Fig. 1. St. Louis firehouse, Circa 1920

buildings with wood roofs and floors was failure of the out-of-plane connections between the perimeter masonry and panelized plywood roofs (Hamburger and McCormick 1994). A report by Bruneau (1994) identified that most of the failures due to earthquakes found in URM buildings during the last 20 years are related to diaphragms and their connections to the walls. These concerns are addressed in this study by including representative connections in the experimental testing of the diaphragms.

The research presented in this paper was part of the Mid-America Earthquake (MAE) Center research program evaluating the lateral in-plane behavior of existing and rehabilitated wood diaphragms in pre-1950s URM buildings found in the Central and Eastern regions of the United States. The work was divided into three tasks: experimental testing of three diaphragm systems rehabilitated using several commonly used methods; development of nonlinear analytical models to represent the important features of the measured response; and development of a simple model to predict the nonlinear lateral response of existing and rehabilitated wood diaphragms of selected length-to-width aspect ratios. The complete study is documented by Peralta et al. (2003). This paper

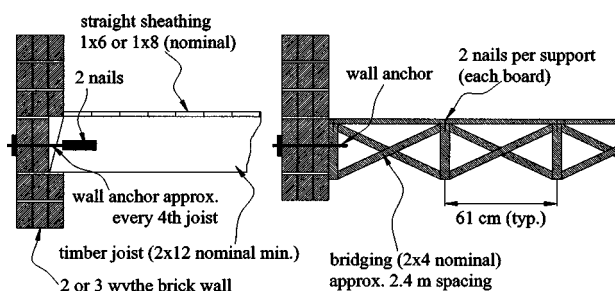


Fig. 2. Typical floor connection details in pre-1950s URM buildings in St. Louis

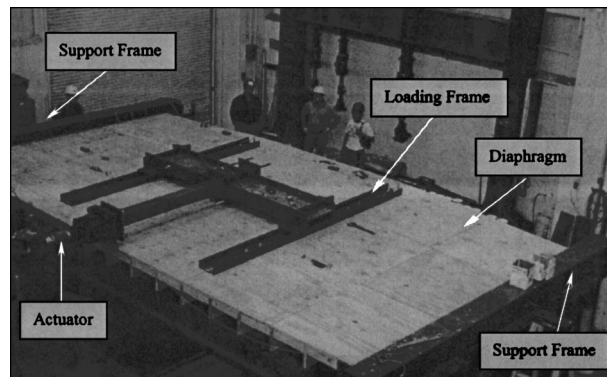


Fig. 3. Experimental setup

summarizes the results of the experimental program and compares them with the predictions of lateral diaphragm response provided in the FEMA 273 guidelines (ATC 1997a, b) and its update, the FEMA 356 guidelines (ASCE 2000). The study provides new and significant information on the behavior of existing and rehabilitated wood diaphragms based on experimental testing. More accurate information on the behavior of wood diaphragms helps describe key parameters for evaluating and retrofitting similar wood diaphragms in older URM buildings, which are very vulnerable to earthquake damage.

Experimental Program

Overview

A general view of the experimental test setup for a diaphragm specimen is shown in Fig. 3. The diaphragm specimens were composed of Southern Pine wood elements and were 7.32 m by 3.66 m in plan. Two steel frames provided gravity and lateral support along the short edges of the specimens parallel to the loading direction. Table 1 gives an overview of the diaphragm specimens. A brief description of each specimen and its retrofits is also provided below. It is important to note that a diaphragm retrofit must consider the impact of retrofit on the overall structural performance. This study focuses on diaphragms alone; therefore the retrofit strategies are based on adding stiffness and strength to the existing diaphragms based on the results of the diaphragm specimen behavior. Additional details may be found in the report by Peralta et al. (2003).

Lateral displacements were applied using one actuator connected to an H-shaped steel loading frame attached at the third points along the diaphragm width. Displacement-controlled quasi-static reverse cyclic testing was performed for each diaphragm applying two cycles for each displacement amplitude ranging from ± 3.2 to ± 76.2 mm. The response of the specimen was monitored during the test with 12 displacement transducers (LVDTs) and four strain gauges. Most of the instruments were located along the long side of the diaphragm opposite to the actuator location.

Specimen 1: Existing and Retrofits

Diaphragm MAE-1 represents a floor with 1x4 nominal (19 mm x 89 mm) by 3.66 m tongue and groove (T&G) sheathing running in the short direction. A plan view of half of the diaphragm and typical connection details are given in Fig. 4. The

Table 1. Diaphragm Specimen Description

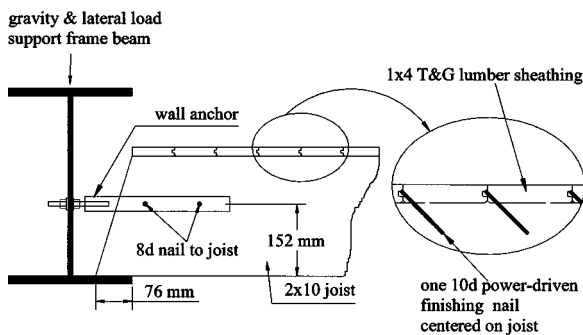
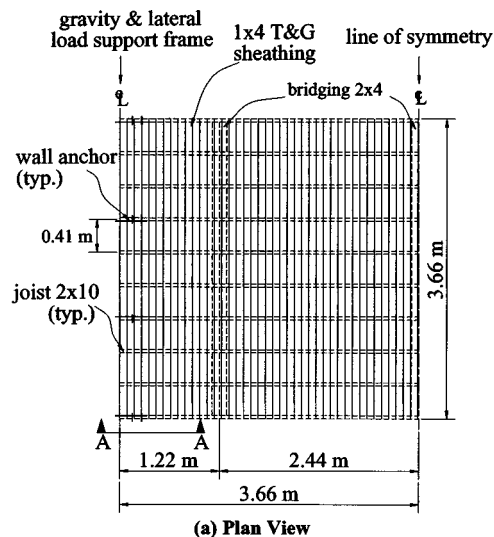
Diaphragm	Description
MAE-1	1×4 tongue and groove (T&G) sheathing, star anchors
MAE-1A	MAE-1 with enhanced bolted connections and perimeter steel strapping
MAE-1B	MAE-1A with steel truss
MAE-2	1×6 straight sheathing, bolted connections, unchorded
MAE-2A	MAE-2 with steel truss
MAE-2B	MAE-2 with 9.5 mm unblocked plywood overlay
MAE-2C	MAE-2 with 9.5 mm blocked plywood overlay
MAE-3	1×6 straight sheathing, bolted connections, unchorded, corner opening
MAE-3A	MAE-3 with 9.5 mm unblocked plywood overlay
MAE-3B	MAE-3 with 9.5 mm blocked plywood overlay, steel strap at opening

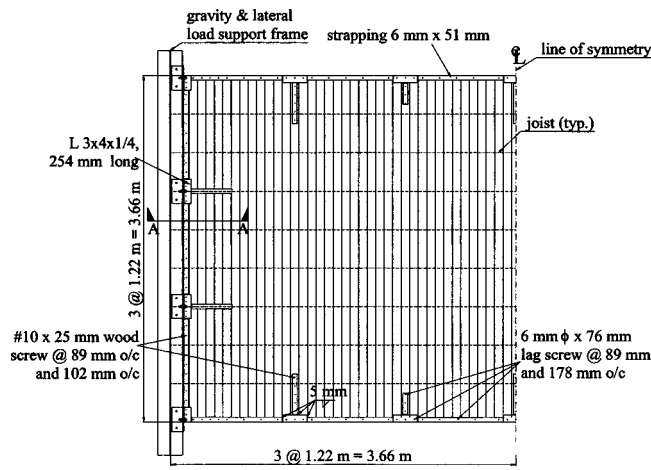
T&G sheathing was secured to supporting beam joists using power-driven blind-nailing (nails toe-nailed through the tongue) at every intersection with one 10d finishing head type nail per beam joist. The framing structure was composed of an arrangement of 2×10 nominal (38 mm×235 mm) by 7.32 m beam joists running in the long direction and spaced 406 mm on center. Bridging members composed of 2×4 nominal (38 mm×89 mm) angled boards were placed in rows spaced at 2.43 m, toe-nailed between the beam joists with two 8d common wire

nails at each end. Replica wall anchors attached the framing to the steel support frames at every fourth beam joist, giving a total of four anchors for each support frame. Steel anchors were fabricated in the laboratory to replicate wall anchors found in pre-1950s URM construction.

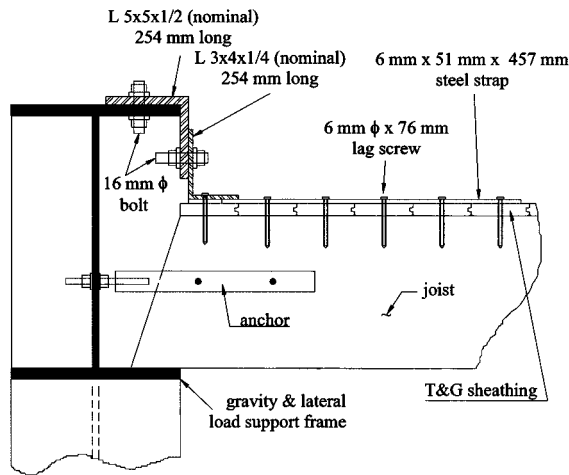
Based on the experimental results for specimen MAE-1 and historical seismic performance of wood diaphragms in URM buildings, the first retrofit (MAE-1A) was designed to improve the attachment between the diaphragm and the lateral load support system. A plan view of half of the diaphragm and connection details are given in Fig. 5. A steel strap was added around the diaphragm perimeter and additional bolted connections were provided to the lateral support. The steel strap was added to act as a chord and to improve the shear transfer between the diaphragm and the support frame through the existing and added connections. The cross-sectional dimensions of the steel strap were 51 mm by 6.4 mm. The perimeter straps running in the joist direction (long direction of the diaphragm) were attached to the decking and joists with 6 mm ϕ ×76 mm long lag screws spaced every 178 mm. The perimeter straps running perpendicular to the joists were attached every 102 mm using No. 10×25 mm long wood screws and one 6 mm ϕ ×76 mm lag screw on every joist intersection. A 3×4×1/4 (nominal) by 254 mm long steel angle was connected to the lateral support frame with one 16 mm ϕ ×38 mm bolt and to the perimeter strap and diaphragm with four No. 10×25 mm wood screws every 51 mm and one 16 mm ϕ ×76 mm lag screw to the joist.

The second retrofit, MAE-1B, was designed to significantly increase the diaphragm stiffness and shear capacity by attaching a steel truss system to the bottom of the diaphragm joists. A plan view of half of the diaphragm is given in Fig. 6. The truss was designed using the AISC-LRFD code. All eight members of the truss were WT4×6.5 (US) sections, oriented with the flange against the underside of the beam joists. The ends of the truss members were bolted to gusset plates with four 16 mm bolts. The gusset plates were 6 mm thick and attached to the wood joists with 8 mm ϕ ×76 mm lag screws spaced every 51 mm. For reasons of construction time and cost, the truss configuration was not cross braced in the middle. The bracing was not required on the specimen because the lateral loading was applied directly on top of the collector elements parallel to the loading. However, cross bracing would be necessary when applying this retrofit to a URM building, where bidirectional or asymmetric loading needs to be considered.

**(b) Section A-A Connection and Nail Details****Fig. 4.** MAE-1: Tongue and groove sheathed diaphragm



(a) Plan View Details



(b) Section A-A - Connection Detail

Fig. 5. MAE-1A: Chord and connection retrofit

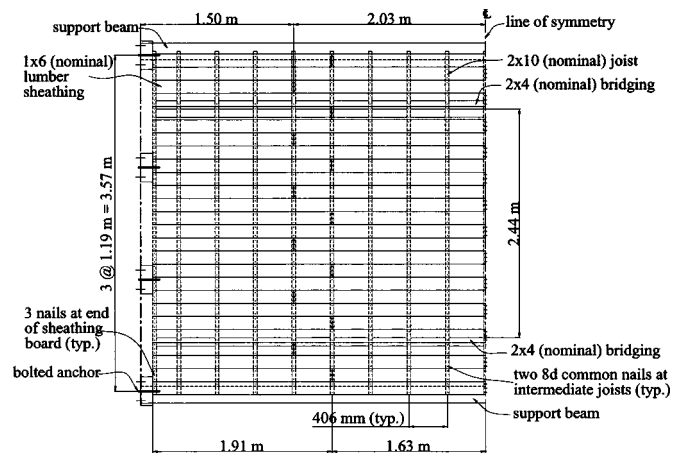


Fig. 7. MAE-2: Straight sheathed diaphragm

Specimen 2: Existing and Retrofits

Diaphragm specimen MAE-2 was designed to represent a typical flat roof or floor diaphragm with square edged straight sheathing boards. A plan view is shown in Fig. 7. The sheathing boards were 1×6 nominal (19 mm×140 mm) square edged boards running staggered in the long direction of the diaphragm and nailed to the joists with two 8d common nails at each joist intersection and three 8d common nails where the end of each board connected to the supporting joist. The joists were 2×10 nominal (38 mm×235 mm) by 3.66 m boards spanning in the short direction with bridging similar to diaphragm MAE-1. Threaded steel bars, 16 mm in diameter by 254 mm long, were used to anchor the specimen to the steel support frames by passing through the edge joists at their midheight every 1.22 m.

As will be discussed later, the existing diaphragm was quite flexible. Therefore the three retrofits were selected to reduce lateral displacements. The first retrofit (MAE-2A) consisted of a steel truss, as used for diaphragm MAE-1, with some minor modifications and with the same purpose of significantly increasing the lateral stiffness of the diaphragm.

For specimen MAE-2B, the steel truss from the diaphragm was removed and an unblocked plywood overlay was nailed to

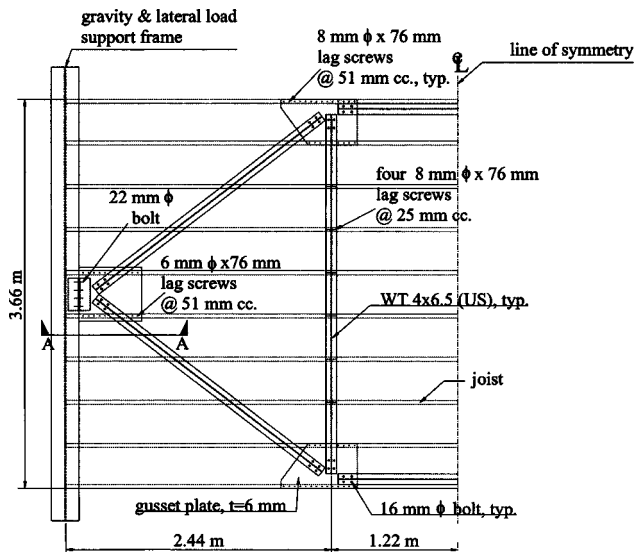


Fig. 6. MAE-1B: Steel truss retrofit (sheathing not shown for clarity)

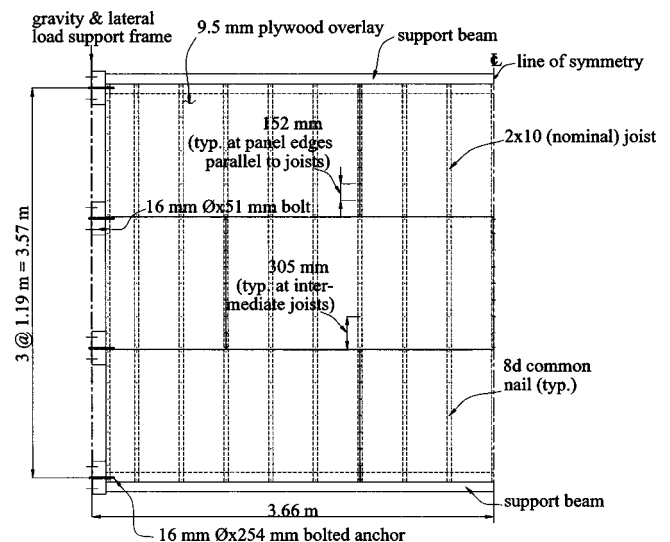


Fig. 8. MAE-2B: Unblocked plywood overlay retrofit

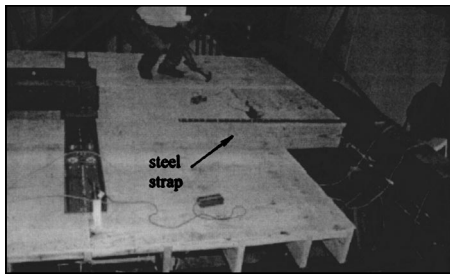


Fig. 9. MAE-3B: Blocked plywood overlay retrofit

the diaphragm to improve the in-plane lateral stiffness of the diaphragm. A plan view of half of the diaphragm is given in Fig. 8. The design was based on provisions from APA (Tissell and Elliott 1997). The thickness of the plywood overlay was 9.5 mm and the panels were arranged as shown in Fig. 8. The panels were nailed with 8d common nails at 152 mm spacing along the supported edges and 305 mm spacing along intermediate joists. A gap of 3 mm was left between panels along all edges in accordance with APA plywood sheathing installation recommendations (APA 1985).

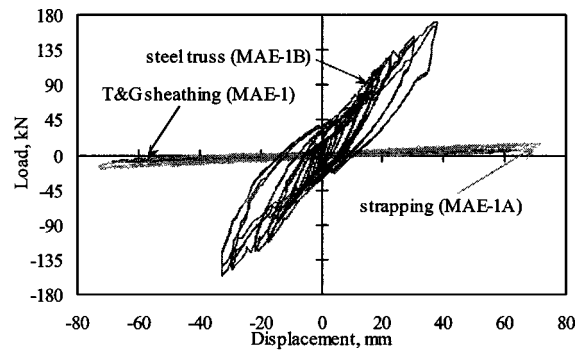
The third retrofit, labeled MAE-2C, had additional blocking members (composed of toe-nailing 2×4 boards between the joists below the panel edges) and additional nailing so the panels were nailed in the long direction every 51 mm at the diaphragm boundaries and every 76 mm at the other panel edges (both directions). The nail spacing followed the provisions from APA (Tissell and Elliott 1997). No additional nails were added along the intermediate supporting joists.

Specimen 3: Existing and Retrofits

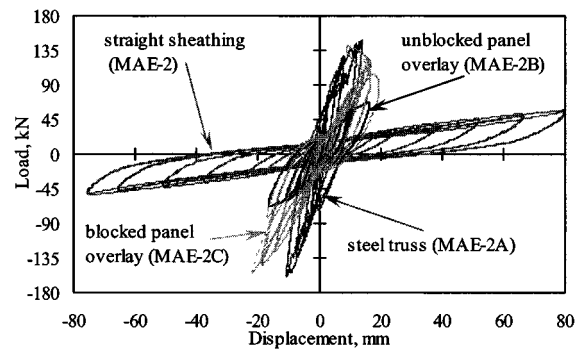
The geometry, construction, and materials used in diaphragm specimen MAE-3 were similar to diaphragm MAE-2 with the addition of a 0.81 m by 1.57 m opening located at one corner of the diaphragm, to represent a stairwell opening. Two joists were shortened and nailed to a transverse 1.57 m long joist to frame the opening. The sheathing was also shortened at the required locations and the boards were staggered appropriately. Along the diaphragm edge with the opening only three anchors were used to attach the diaphragm to the support frame.

Diaphragm MAE-3 was first retrofitted with an unblocked plywood panel overlay (MAE-3A) similar to diaphragm MAE-2B. Plywood panels of 9.5 mm thickness and 1.22 m by 2.44 m in plan were nailed using 8d common nails. The nail arrangement consisted of 152 mm spacing on the supported panel edges parallel to the loading and 305 mm spacing at the interior joists. A gap of 3 mm was used between panels in both directions.

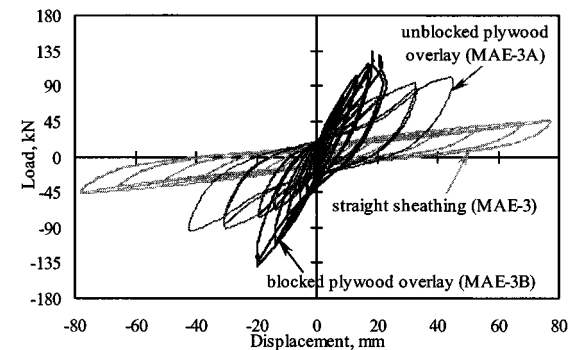
The second retrofit, MAE-3B, had additional 2×4 blocking boards placed adjacent to the bottom face of the sheathing and running below the unsupported edges of the plywood panels. The blocking boards were toe-nailed to the joists using 8d common nails. With the blocking in place, nails were added to reduce the nail spacing to 51 mm along the edges of the diaphragm and 76 mm at the other panel edges. Additionally, a $6 \text{ mm} \times 51 \text{ mm} \times 1.52 \text{ m}$ steel strap was attached on top of the diaphragm, along the short side of the opening to reinforce the corner. Blocking boards were added between joists and nailed to the joists to secure the steel strap with $8 \text{ mm } \phi \times 76 \text{ mm}$ lag screws spaced every 51 mm. A photo of diaphragm MAE-3B, showing the opening, is provided in Fig. 9.



(a) Specimen 1: Existing and Retrofits



(b) Specimen 2: Existing and Retrofits



(c) Specimen 3: Existing and Retrofits

Fig. 10. Cyclic response of diaphragm specimens

Experimental Results

Specimen 1: Existing and Retrofits

The cyclic response of Specimen 1 (existing and retrofits) is shown in Fig. 10(a). Specimen MAE-1 displayed flexible in-plane behavior during lateral loading. Failure of the diaphragm was not reached through the maximum actuator stroke ($\pm 76 \text{ mm}$). Since the T&G sheathing did not have a nail couple in their connection to the supporting joists, the lateral resistance of the diaphragm was primarily attributed to bending of the joists and friction between the T&G sheathing. There were no signs of damage to the wood components or anchor connections at the completion of testing with in-plane diaphragm drifts up to 2% (maximum midspan displacement divided by one-half the span). The lack of damage was attributed to the high flexibility of the diaphragm, which allowed high deformations under small loads. At peak lateral displacement (71 mm), the lateral displacement (slip) of the anchor connections was 10 mm (14% of total midspan displacement).

The first retrofit (MAE-1A) increased both the strength and stiffness of the diaphragm by a factor of 2, but still did not fail for the maximum applied displacement of 76 mm. The increase in shear strength came from the lag screws used to secure the longitudinal strapping in the sheathing boards and also from the additional bolted connections. The lateral displacement at the anchor connections was reduced to 5 mm (7% of total midspan displacement).

The second retrofit, MAE-1B, with the addition of a steel truss, significantly increased the stiffness and strength of the diaphragm. The high lateral loads generated an overturning moment (from the vertical eccentricity between the actuator, sheathing, and the steel truss), which tended to twist the joists about their longitudinal axes. The test was stopped at 38 mm of displacement amplitude, when major out-of-plane bending cracks appeared in the upper portion of the joist webs, near the T&G sheathing. No sign of damage was observed in the truss members and connections and in the T&G sheathing of nailed connections. The maximum measured lateral displacement of the anchor connection was 4 mm (10% of total midspan displacement).

Specimen 2: Existing and Retrofits

The cyclic response of Specimen 2 (existing and retrofits) is shown in Fig. 10(b). The lateral behavior of specimen MAE-2 was governed by the stiffness of the square edged straight sheathing and the nail couple developed in the nailed connections joining the sheathing to the supporting joists. At the imposed peak displacement (76 mm), the lateral slip displacement measured at the anchor connection was 1.3 mm (1.6% of total midspan displacement). No cracks were detected in the joists or sheathing and permanent deformation of the nailed connections was not visible.

The steel truss retrofit (MAE-2A) significantly increased the strength and stiffness of the diaphragm. The test was stopped at 13 mm of displacement amplitude when one edge of the diaphragm lifted off the gravity supports located along the long edges. The diaphragm uplift was caused by the overturning moment due to the vertical eccentricity between actuator load and the center of resistance of the diaphragm and truss system. The maximum lateral displacement was 1.8 mm at the anchor connection (13% of total midspan displacement). No visible damage was observed for the sheathing boards, nailed connections, joists, or anchor connections.

The second retrofit, an unblocked plywood panel overlay (MAE-2B), showed an intermediate behavior between the unretrofitted case and the steel truss retrofit. The test was terminated at 19 mm of displacement amplitude because of buckling of a corner plywood panel. The lateral displacement at the connection was 2.3 mm (14% of total midspan displacement). No further signs of damage were observed in the diaphragm. The failure occurred at a relatively low level of load because the panel nails, at fairly wide spacing, pulled through the plywood overlay.

Testing of the diaphragm retrofitted with blocked plywood panel overlay (MAE-2C) showed an increase in strength and stiffness. At 12.7 mm of applied displacement, small cracks developed in the plywood panels adjacent to the support frames. At 19 mm, large bearing cracks developed in the joist ends near the anchor connections. At 25 mm, the overturning moment started the uplift of one edge of the diaphragm. The test was stopped at the next cycle (38 mm) when the diaphragm uplift increased. The lateral displacement was 6.6 mm (33% of total midspan displacement) at the anchor connections.

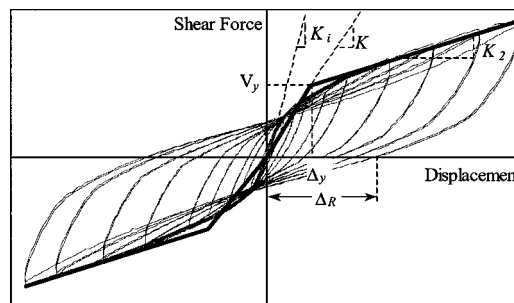


Fig. 11. Cyclic response of diaphragm specimens

Specimen 3: Existing and Retrofits

The cyclic response of Specimen 3 (existing and retrofits) is shown in Fig. 10(c). The behavior of diaphragm MAE-3 and its retrofits MAE-3A and MAE-3B was similar to that for diaphragms MAE-2, MAE-2B, and MAE-2C, respectively; but the addition of a corner opening for MAE-3 resulted in a lower strength and stiffness. Diaphragm MAE-3 was tested for displacement amplitudes up to the maximum actuator stroke of 76 mm. The maximum lateral displacement at the anchor connection was 2 mm (2.5% of total midspan displacement). The effect of the diaphragm opening is apparent in the load-displacement curves, where the load is, on average, 16% lower than the values for diaphragm MAE-2 for a given value of displacement. The elements surrounding the diaphragm opening did not show signs of permanent large deformation or failure. No visible damage was found in the joists, sheathing boards nails, or anchor connections.

Diaphragm MAE-3A, the addition of the unblocked plywood overlay to diaphragm MAE-3, had a maximum lateral displacement at the midpoint of 49 mm. The displacement at the anchor connections was 5 mm (10% of total midspan displacement). The test was terminated when nails from panels adjacent to the support frames of the diaphragm pried out.

For blocked diaphragm MAE-3B, the maximum lateral displacement at midpoint was 33 mm. The corresponding lateral displacement at the anchor connections was 13 mm (40% of total midspan displacement). The test was terminated after an overturning moment developed in the diaphragm lifting up the diaphragm edge opposite to the actuator. No nails pried out from the top of the diaphragm and no visible damage was observed around the opening, panel overlay, or nails. MAE-3B developed long bearing cracks in the joists at the anchor connections at 25 mm of applied displacement. No visible damage was observed around the corner opening, panel overlay, or in the nailed connections.

Comparison of Measured and Predicted Behavior

Bilinear Representation of Experimental Response

The essential features of the in-plane lateral force-displacement response of the wood diaphragm specimens are illustrated in Fig. 11. Idealized lateral force versus deformation pushover curves (backbone curves) were developed from the measured response at the diaphragm midpoint by plotting a series of linear segments through the intersection of the first cycle curve for the (i) th deformation step with the second cycle curve of the $(i-1)$ th deformation step, for all steps based on the procedure outlined in FEMA 273 (ATC 1997a).

Table 2. Parameters for Bilinear Representation of Experimental Data

Diaphragm	Yield load V_y (kN)	Yield displacement Δ_y (mm)	Effective stiffness K (kN/cm)	Postyield stiffness	
				K_2 (kN/cm)	% K
MAE-1	3.6	25	1.4	0.9	64%
MAE-1A	7.1	15	5.1	1.3	25%
MAE-1B	116	20	59	29	48%
MAE-2	29	16	18	4.0	22%
MAE-2A	115	5.1	233	54	23%
MAE-2B	48	5.8	84	18	22%
MAE-2C	68	5.8	113	55	49%
MAE-3	23	12	19	3.5	19%
MAE-3A	65	13	51	6.7	13%
MAE-3B	82	12	71	29	41%

Bilinear representations were constructed from the measured backbone curves by defining an equivalent bilinear system with the same energy absorption as the real system (Mahin and Bertero 1981), as described in FEMA 273. For the construction of the bilinear representation, the regions under the bilinear curve and the measured backbone curve have the same area. The intersection of the segments in the bilinear curve defines the yielding point. The yield displacement (Δ_y), yield load (V_y), effective stiffness (K), and postyield stiffness (K_2) were calculated from the equivalent bilinear curves. It should be noted that the adopted criterion for the bilinear curve does not accurately represent the postyield stiffness because it does not reflect the reduction in the measured strength with increasing displacement amplitudes. However, this model was used for consistency with the recommendations given in FEMA 273. The parameters for the bilinear curves of the experimental data are provided in Table 2.

Predicted Response

General

The predicted bilinear curves, determined using the former and current FEMA guidelines, are composed of the effective stiffness, the lateral yield shear strength, and the postyield stiffness. A brief description of the procedures and values given by the FEMA guidelines to determine these parameters is given below. The lateral yield load, which is the applied load required to initiate yielding of the diaphragm and equal to twice the lateral yield shear strength, is used for ease of comparison with the experimental results. The predicted values of effective stiffness and lateral yield load are summarized in Table 3.

Effective Stiffness

The effective stiffness values for all specimens are summarized in Table 3 for both the FEMA 273 (ATC 1997a) and the FEMA 356 (ASCE 2000) guidelines. FEMA 273 provides a single equation to calculate the lateral deflection for straight-sheathed diaphragms with or without plywood panel overlays. From this equation, an expression for the effective stiffness K was obtained as follows:

$$K = 2G_d \left(\frac{b}{L} \right)^4 \tag{1}$$

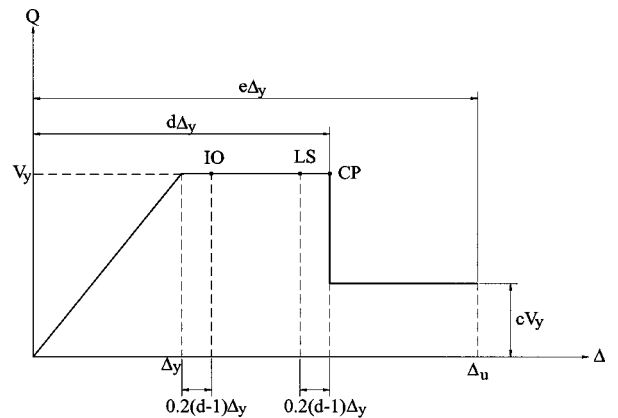
where L =diaphragm span between shear walls or collectors (7.32 m), b =diaphragm width (3.66 m for MAE-1 and MAE-2, 2.9 m for MAE-3), and G_d =diaphragm shear stiffness from FEMA 273 (in kN/m) listed in Table 3.

FEMA 356 provides the following expression for the effective stiffness:

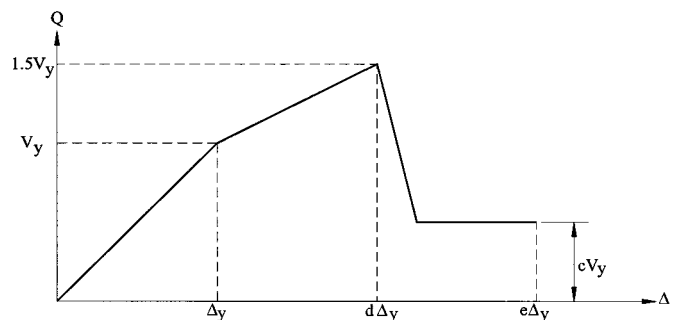
$$K = \frac{4bG_d}{L} \tag{2}$$

where the terms in this equation are the same as for Eq. (1), but the diaphragm shear stiffness values are now taken from FEMA 356 and are listed in Table 3.

The FEMA guidelines do not provide recommendations for T&G sheathed diaphragms. For this reason, the specifications for straight-sheathed diaphragms were used to determine the pre-



(a) FEMA 273



(b) FEMA 356

Fig. 12. Simplified backbone curve for wood diaphragms (adapted from FEMA 273 and FEMA 356)

J. Struct. Eng. 2004.130:2046-2050. Downloaded from ascelibrary.org by David Peralta on 07/13/12. For personal use only. No other uses without permission. Copyright (c) 2012. American Society of Civil Engineers. All rights reserved.

Table 3. Predicted Effective Stiffness and Lateral Yield Load

	Shear stiffness G_d (kN/cm)		Effective stiffness K (kN/cm)		Lateral yield load (kN)	
	FEMA 273	FEMA 356	FEMA 273	FEMA 356	FEMA 273	FEMA 356
Diaphragm	273	356	273	356	273	356
MAE-1	351	3.51	43.8	7.0	6.0	4.5
MAE-1A	351	3.51	43.8	7.0	11.7	8.7
MAE-1B	—	—	933	—	352	—
MAE-2	351	3.51	43.8	7.0	12.9	12.9
MAE-2A	—	—	933	—	352	—
MAE-2B	877	8.77	110	17.5	32.0	32.0
MAE-2C	1,230	12.3	153	24.5	72.8	96.9
MAE-3	351	3.51	17.2	5.6	10.2	10.2
MAE-3A	877	8.77	43.0	13.9	25.4	25.4
MAE-3B	1,230	12.3	60.2	19.4	57.6	76.7

dicted response. In the case of the diaphragm specimens with a corner opening (MAE-3, MAE-3A, and MAE-3B), a reduction of stiffness and lateral yield load was expected due to the discontinuity and the reduced width of the diaphragm. To account for this discontinuity, an average diaphragm width of 2.9 m was used as an approximation to determine the predicted response using the guidelines for diaphragms with no openings. The effective stiffness of the steel truss retrofit was calculated based only on the axial deformations of the truss members.

Lateral Yield Shear Strength

FEMA 273 Predictions The lateral yield shear strength of the T&G diaphragm (specimen MAE-1) was estimated by summing the shear strength of the nails connecting the sheathing board to the framing across the diaphragm width (10 nailed connections). The yielding shear force of the nail was determined using the allowable shear strength for a nail (Z') equal to 0.1 kN, calculated as described in the National Design Specification for Wood Construction (NDS) (AF&PA 1997) multiplied by a factor of 2.8 as per FEMA 274 (ATC 1997b) for single straight-sheathed diaphragms. The resulting lateral yield shear strength for this diaphragm is 3 kN, or a lateral load of 6 kN is required to start yielding of the diaphragm.

For the first retrofit of the T&G diaphragm, specimen MAE-1A, the additional shear strength of the retrofit was provided by the lag screws that attached the steel straps to the framing. From NDS, an allowable shear design value for a lag screw (Z') equal to 0.5 kN was calculated. Two lag screws per sheathing board were considered to compute the additional shear. Using the factor of 2.8 from FEMA 274 to determine the lateral yield shear strength, the additional yield shear strength provided by the lag screws is equal to 2.8 kN. The resulting lateral yield load for diaphragm MAE-1A was 11.8 kN.

For straight-sheathed diaphragms with two or more nails at each sheathing board to joist connection (diaphragm specimens MAE-2 and MAE-3), the FEMA 273 guidelines provide a diaphragm yield shear strength per diaphragm width (v_y) of 1.8 kN/m. A lateral yield load of 12.8 kN was determined for diaphragm MAE-2 and 10.2 kN for diaphragm MAE-3.

For the case of unblocked, unchorded plywood panel overlays on straight-sheathed diaphragms (specimens MAE-2B and MAE-3A), FEMA 273 provides a typical yield shear strength per dia-

phragm width of 4.4 kN/m. The corresponding predicted lateral yield load is 32.0 and 25.4 kN for diaphragms MAE-2B and MAE-3A, respectively.

For blocked, unchorded plywood panel overlays on straight-sheathed diaphragms (specimens MAE-2C and MAE-3B), FEMA 273 suggests a yield shear capacity of 1.5 times the allowable shear capacity of a comparable plywood structural panel diaphragm without existing sheathing. Tissel and Elliott (1997) provide a design table for horizontal plywood diaphragms with Southern Pine framing for seismic loading. The corresponding tabulated value including reduction factors gave an allowable shear capacity of 6.6 kN/m. The resulting predicted yield shear strength per diaphragm width is 10.0 kN/m. The corresponding predicted lateral yield load is 72.8 kN for diaphragm MAE-2C and 57.6 kN for diaphragm MAE-3B.

FEMA 356 Predictions The procedure provided in FEMA 356 for predicting the lateral yield shear strength is based on design resistance values associated with the LRFD code for wood (AF&PA/ASCE 1995). The lateral yield shear strength for the T&G diaphragms (specimens MAE-1 and MAE-1A) was calculated from the allowable shear of the nailed or lag screw connection, as was done for FEMA 273. All adjustment factors were considered except for the load duration factor. Instead, the time-effect factor is included. For earthquake loads, the value of this factor is 1.0. The same allowable design lateral values (Z') used for FEMA 273 were used, multiplied by a format conversion factor (K_E) equal to 3.32 and divided by the load duration factor (C_D) equal to 1.6 for nails and lag screws, resulting in a factor of 2.08. The following equation gives the relationship between the FEMA 356 and FEMA 273 predicted yield shear strengths:

$$Z'_{\text{FEMA 356}} = 2.08Z'_{\text{FEMA 273}} \quad (3)$$

The corresponding predicted lateral yield load for FEMA 356 is 4.5 kN for MAE-1 and 8.7 kN for MAE-1A.

FEMA 356 has the same values given in FEMA 273 for the lateral yield shear strength for straight-sheathed diaphragms (specimens MAE-2 and MAE-3) and unblocked panel overlays on straight-sheathed diaphragms (specimens MAE-2B and MAE-3A). The yield shear capacity for blocked plywood panel overlay on straight-sheathed diaphragms can be calculated without the contribution of the straight sheathing. The "LRFD Manual for

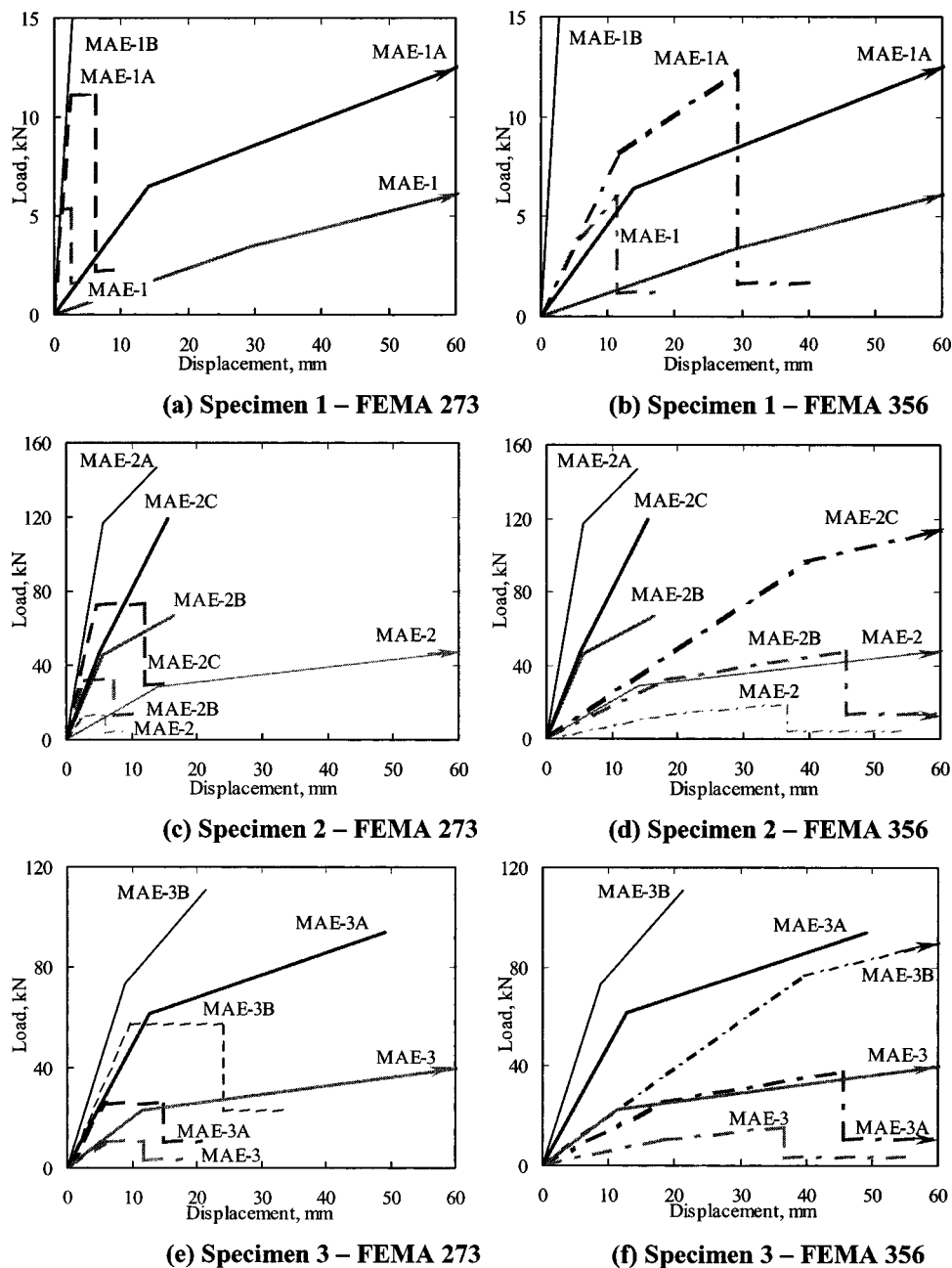


Fig. 13. Comparison of FEMA backbone curves and bilinear curves

Engineered Wood Construction" (AF&PA 1996), which is to be used in conjunction with AF&PA/ASCE (1995), provides a table of factored shear resistance for structural-use panel horizontal diaphragms with Southern Pine framing for seismic loading. A factored yield shear capacity of 11.4 kN/m was found from the table. Reduction factors of 0.89 and 0.85 should be applied to consider the use of 51 mm nominal width of framing and 51 mm nail spacing at the boundary. Additionally, it is necessary to divide by the resistance factor ϕ equal to 0.65 for connections. The predicted yield shear strength per unit width is 13.3 kN/m. The predicted lateral yield load is 96.9 kN for diaphragm MAE-2C and 76.7 kN for diaphragm MAE-3B.

The FEMA guidelines provide simplified backbone curves to determine an idealized in-plane nonlinear force versus deformation relationship for wood diaphragms. Fig. 12 shows samples of force versus deformation curves for both guidelines. Table 4 lists

the yield displacement and nondimensional parameters c , d , and e given in the FEMA guidelines for each type of diaphragm. Distance d is considered to be the maximum deformation ratio of the diaphragm at the point of first loss of strength. Distance e is the maximum deformation ratio at a reduced shear strength ratio c .

Comparison

Fig. 13 shows a single quadrant of the bilinear representations from the measured response and the predicted bilinear representations from FEMA 273 (left side) and its update FEMA 356 (right side) for the diaphragm specimens. The horizontal and vertical axes represent the midspan displacement and the lateral load, respectively. From Figs. 13(a) and 13(b), it can be observed that the predicted backbone curves provided a poor estimate of the measured bilinear curves for Specimen 1 diaphragms MAE-1 and

Table 4. Parameters of Predicted Backbone Curves of Diaphragm Specimens

Diaphragm	Δ_y (mm)		c^c	d^c	e^c
	FEMA 273 ^a	FEMA 356 ^b			
MAE-1	1.3	5.6	0.3	2.0	3.0
MAE-1A	2.5	11.7	0.2	2.5	3.5
MAE-1B	3.8	—	—	—	—
MAE-2	3.0	18.3	0.3	2.0	3.0
MAE-2A	3.8	—	—	—	—
MAE-2B	3.0	18.3	0.4	2.5	3.5
MAE-2C	4.8	39.6	0.4	2.5	3.5
MAE-3	5.8	18.3	0.3	2.0	3.0
MAE-3A	5.8	18.3	0.4	2.5	3.5
MAE-3B	9.6	39.6	0.4	2.5	3.5

^aUsing Eq. (1).^bUsing Eq. (2).^cFrom the FEMA 273 and 356 guidelines (same for both).

MAE-1A, especially the effective stiffness (K) values. However, it should be noted that FEMA 273 and FEMA 356 do not provide values for T&G sheathed diaphragms and values for straight-sheathed diaphragms were used instead, which helps to explain the poor estimate. Figs. 13(c) and 13(d) compare the results for Specimen 2 diaphragm and retrofits. In general, FEMA 273 over-predicted the stiffness and significantly underpredicted the yield displacement and ultimate deformation levels. FEMA 356, on the other hand, underpredicted the stiffness and overpredicted yield displacement. Comparing the results for Specimen 3 diaphragms in Figs. 13(e) and 13(f), the results from FEMA 273 gave closer stiffness predictions but still underpredicted the yield displacement and deformation levels for MAE-3 and MAE-3A. Again, FEMA 356 underpredicted stiffness and overpredicted the yield displacement. For the existing diaphragm cases, FEMA 356 underpredicted the ultimate deformation. However, it is difficult to evaluate how well FEMA 356 predicted ultimate deformations for the retrofitted specimens because the testing was terminated at lower displacements due to some uplift that resulted from the testing configuration.

It should be noted that the specimens in the experimental program were built of new materials with properly tightened connections. However, the actual lateral response of pre-1950s diaphragms might be different than those in the experimental program due to material aging, deterioration, and connection degradation. This may be the cause of the deviation between the experimental response and the predicted response based on the updated FEMA 356 guidelines. However, the updated FEMA 356 guidelines tend to conservatively estimate the diaphragm response in terms of strength, stiffness, and deformability. Further experimental studies should be conducted to consider the effects of time and decay on the diaphragm response.

Conclusions

The lateral in-plane behavior of wood diaphragms, replicating several details of pre-1950s construction, was determined from experimental tests using quasi-static reverse cyclic loading. Test results show that the four rehabilitation methods used (steel strapping and enhanced shear connections, steel truss, unblocked and blocked wood panel overlays) accomplished the objectives of increasing in-plane lateral shear strength and stiffness. The steel

truss retrofit provided the largest increase in shear strength and stiffness, followed by the blocked plywood panel overlay retrofit. Measured deformations of the prototype diaphragm-to-wall anchor connections indicate that these connections can contribute to the overall lateral displacements of the diaphragms by up to 13%. Backbone curves for the diaphragm specimens based on the experimental measurements were not predicted with accuracy when using the recommendations in FEMA 273 and its update FEMA 356. For the diaphragms tested, FEMA 273 tended to overpredict the stiffness and significantly underpredict yield displacement and deformation levels, while FEMA 356 tended to underpredict stiffness and overpredict yield displacement. However, the updated FEMA 356 guidelines tend to conservatively estimate the diaphragm response in terms of strength, stiffness, and deformability.

Acknowledgments

The writers wish to acknowledge the National Science Foundation and the University of Illinois who funded this research through the Mid-America Earthquake Center (NSF Grant No. EEC-9701785). The financial support provided by the Civil Engineering Department and the Texas Engineering Experiment Station at Texas A&M University, where this research was conducted, is also appreciated. The opinions expressed in this paper are those of the writers and do not necessarily reflect the views or policies of the sponsors.

Notation

The following symbols are used in the paper:

- b = diaphragm width;
- C_D = load duration factor;
- c = nondimensional parameter;
- d = nondimensional parameter;
- e = nondimensional parameter;
- G_d = diaphragm shear stiffness;
- K = effective stiffness;
- K_E = format conversion factor;
- K_2 = postyield stiffness;
- L = diaphragm span;

- V_y = yield load;
 v_y = diaphragm yield strength per diaphragm width;
 Z' = allowable shear strength per nail or lag screw;
 Δ_u = ultimate displacement; and
 Δ_y = yield displacement.

References

- American Forest & Paper Association (AF&PA). (1996). *LRFD manual for engineered wood construction*, Washington, D.C.
- American Forest & Paper Association (AF&PA). (1997). *National design specification for wood construction*, NDS, Washington, D.C.
- American Forest & Paper Association/American Society of Civil Engineers (AF&PA/ASCE). (1995). "Standard for load and resistance factor design (LRFD) for engineered wood construction." *AF&PA/ASCE 16-95*, Reston, Va.
- American Society of Civil Engineers (ASCE). (2000). "Prestandard and commentary for the seismic rehabilitation of buildings." *FEMA Publication 356*, Federal Emergency Management Agency, Washington, D.C.
- APA—The Engineered Wood Association (APA). (1985). *Design/construction guide—Residential and commercial*, Tacoma, Wash.
- Applied Technology Council (ATC). (1997a). "NEHRP guidelines for the seismic rehabilitation of buildings." *FEMA Publication 273*, Building Seismic Safety Council, Washington, D.C.
- Applied Technology Council (ATC). (1997b). "NEHRP commentary on the guidelines for the seismic rehabilitation of buildings." *FEMA Publication 274*, Building Seismic Safety Council, Washington, D. C.
- Bruneau, M. (1994). "State-of-the-art report on seismic performance of unreinforced masonry buildings." *J. Struct. Eng.* 120(1), 230–251.
- Hamburger, R. O., and McCormick, D. L. (1994). "Implications of the January 17, 1994 Northridge Earthquake on tilt-up and masonry buildings with wood roofs." *Northridge Earthquake: Lessons Learned, 1994 SEAONC Spring Seminar*, San Francisco.
- Mahin, S., and Bertero, V. V. (1981). "An Evaluation of inelastic seismic design spectra." *J. Struct. Div. ASCE* 107(9), 1777–1795.
- Peralta, D. F., Bracci, J. M., and Hueste, M. D. (2003). *Seismic performance of rehabilitated wood diaphragms*, Mid-America Earthquake Center, University of Illinois at Urbana-Champaign, CD Release 03-01.
- Stelzer, C. D. (1999). "On Shaky Ground." *St. Louis Riverfront Times*, <www.riverfronttimes.com/issues/1999-12-15/feature.html> (Dec. 15)
- Tissell, J. R., and Elliott, P. E. (1997). "Plywood diaphragms." *Rep. 138*, The Engineered Wood Association (APA), Tacoma, Wash.